New Hamiltonian and Cooper pair's origin of pseudogap and colossal magnetoresistance in manganites

Fu-sui Liu
Department of Physics, Beijing University, Beijing 100871, China
E-mail: fsliu@pku.edu.cn

Abstract

Based on the thirteen similarities of structures of lattice, electron, and strong correlation Hamiltonian between CMR (colossal magnetoresistance) manganites and the high-T_c cuprates, this paper concludes that the Hamiltonian of the high-T_c cuprates and CMR manganites are the same. Based on uniform and quantitative explanations for fifteen experimental facts, this paper concludes that the pseudogap and CMR of manganites are caused completely by formation of Cooper pairs, consisting of two oxygen $2p\sigma$ holes in MnO_2 plane.

PACS numbers: 75.47.Gk; 75.47.Lx; 74.10.+v; 74.72.-z.

Keywords: Pseudogap; Colossal magnetoresistive manganese oxides; Cooper pair; Microscopic superconductivity.

1. Introduction

The manganites known as colossal magnetoresistance (CMR) manganese oxides continue to attract considerable attention due to the presence of CMR and pseudogap [1-19]. The pseudogap of manganites was observed for the first time by Dessau *et al.* in 1998. CMR had been observed in the fifties. Although there were more than fifteen proposed mechanisms on the pseudogap and CMR, no one mechanism can uniformly and quantitatively explain both the pseudogap and CMR, and no one mechanism connects with Cooper pair. CMR and pseudogap have not yet haven widely accepted mechanism. Theory falls behind experiment very far, is still in model stage, phenomenological, and has some obvious mistakes. Let me give you an example on the situation of theoretical studies.

A widely used models of manganites are one- or two-orbital, in which just one or two orbitals of $3de_g$ are considered, respectively (Eqs. (5.7) and (5.11) in Ref. [9]). However, experiments have observed that the itinerant carriers in manganites are doped oxygen $2p\sigma$ holes rather than $3de_g$ electrons [13]. However, at present, the common theoretical view is [9]: "However, adding the oxygen orbitals to the electronic models complicates enormously the theoretical studies, which are already quite difficult even with only Mn sites." It is obvious that the present any theories cannot correctly explain the observed facts on the pseudogap and CMR because both these are directly connect with carriers, and the carriers are 2p holes other than 3d electrons.

The goals in this paper are: (i). To point out thirteen similarities between CMR manganites and the high-T_c cuprates in aspects of lattice, electronic, and Hamiltonian; (ii). To prove the Cooper pair's origin of both pseudogap and CMR of manganites by uniform explanations for the 15 key exper-

imental facts; (iii). To give some applications of CMR manganites at room temperature; (iv). To emphasize the advantages of CMR manganites over superconductors and semiconductors.

2. The thirteen similarities between CMR manganites and high-T_c cuprates

The basic building block of manganites is the MnO_6 octahedron [7]. These octahedrons share their in-plane oxygen atoms, forming two dimensional MnO_2 planes, and in this plane, many effects occur [7]. The Fermi surface in MnO_2 plane has nesting structure [2]. The Mn^{3+} and Mn^{4+} ions are local spins $S = 2$ and $S = 3/2$, respectively [9]. Therefore, in both lattice and electronic structures the manganites and high-Tc cuprates are the same [11].

For the CuO_2 plane of the high-T_c cuprates, the strong correlated Hamiltonian is [21,11]

$$\begin{aligned} H &= t_\circ \sum_{i,\alpha,s} (d^+_{is} p_{\alpha s} + h.c) + U_d \sum_i n_{di\uparrow} n_{di\downarrow} + U_p \sum_\alpha n_{p\alpha\uparrow} n_{p\alpha\downarrow} \\ &+ V_\circ \sum_{i,\alpha} n_{di} n_{p\alpha} + \epsilon_d \sum_i n_{di} + \epsilon_p \sum_\alpha n_{p\alpha}, \end{aligned} \tag{2.1}$$

where d^+_{is} and $p^+_{\alpha s}$ create holes on the Cu:d and O:p orbits at sites i and α with spin $s = 1/2$, respectively, n_{di} ($n_{p\alpha}$) is the number operator of d (p) holes, $n_{di} \equiv n_{di\uparrow} + n_{di\downarrow}$, $n_{p\alpha} \equiv n_{p\alpha\uparrow} + n_{p\alpha\downarrow}$, $-t_\circ$ is the hopping integral for the holes between adjacent Cu:d and O:p orbits, and U_p, U_d, and $V_\circ$ are intra- and interatomic Coulomb repulsion on O:p orbits, Cu:d orbits, and between both orbits, respectively. The site index with an alphabetic letter stands for Cu site and that with a Greek letter stands for the O site in the CuO_2 plane. We use x to stand for the hole number in one unit cell of Cu lattice in the CuO_2 plane. At half-filling, $x = 0$, there exists one e_g hole per Cu site, i.e., Cu^{2+}; and for $x > 0$ extra holes go into O:p orbits and Cu^{2+} is stable under

doping. If we take that the local spins are 2 or 3/2, then Eq. (2.1) becomes the strong correlated Hamiltonian of the MnO_2 planes.

By treating the first term as a perturbation, Ref. [21] derived an effective Hamiltonian, Ref. [11] made simplification, and the last form is

$$\begin{aligned} H &= -\sum_{i\alpha\beta s} T_{\alpha\beta} p^{+}_{\alpha s} p_{\beta s} + J_K \sum_{i\alpha\beta ss'} \widehat{\mathbf{S}}_i \cdot \overrightarrow{\sigma}_{ss'} p^{+}_{\alpha s} p_{\beta s'} + J \sum_{ij(i<j)} \widehat{\mathbf{S}}_i \cdot \widehat{\mathbf{S}}_j \\ &+ H_{hole-phonon} + H_{hole-hole} \\ &\equiv H_{Kinetic} + H_{Kondo} + H_{Heisenberg} + H_{hole-phonon} + H_{hole-hole}, \qquad (2.1)' \end{aligned}$$

where the summation over α and β stands for the oxygen sites around i-th Mn^{3+} site with local spin $S = 2$; $p_{\alpha s}$ annihilates $O_{p\sigma}$ hole with spin s=1/2 at site α; $\widehat{\mathbf{S}}_i$ is the local spin operator of Mn^{3+} at site i; $\overrightarrow{\sigma}$ is Pauli matrix vector; and i and j are the nearest neighbors. $J > 0$ and $J < 0$ are AFM and FM Heisenberg Hamiltonian, respectively.

The Hamiltonian in Eq. $(2.1)'$ has many different points in comparison with the until now widely accepted Hamiltonian of manganites in Eqs. (5.6-11) of Ref. [9]): (i). $-T_{\alpha\beta} \simeq t_\circ$ is the hopping integral between Mn^{3+} and O^{2-} rather than the hopping integral t between Mn^{3+} and Mn^{3+} [9]; (ii). Our Kondo term represents the interaction between the $2p$ hole and the local spins ($S \equiv 2$) of Mn^{3+} ion, rather than that between the electron of $3de_g$ and Mn^{4+} ion with $S = 3/2$. The serious mistakes of the previous Hamiltonian are: (a). In the previous Kondo Hamiltonian, J_K is substituted by Huns energy J_H. We think that this is a conceptual mistake. According to the basic definition, the Hund energy can only exist in an isolated atom or ion. However, the $3de_g$ electron in the Kondo term of one- nd two-orbital Hamiltonians is itinerant; (b). By the way, if we do not take our Kondo coupling constant $J_K(\approx 0.2)$ eV, and instead take Hund energy $J_H(\approx 2)$ eV, then our numerical simulations give, for example, the pseudogap is 1000 eV! (c). In Eq. $(2.1)'$, the Kondo

Hamiltonian is derived rather than a phenomenological term (Refer to Eq. (5.1) of Ref. [9]); (iii). The third term in Eq. $(2.1)'$ can be both FM ($J < 0$) and AFM ($J > 0$) rather than only AFM and a phenomenological term (Refer to Eq. (5.3) of Ref. [9]); If the manganites are in FM state rather than in AFM state, then the "Double-Exchange" FM model gives this term; (iv). The $H_{hole-phonon}$ represents the coupling between $2p$ hole (rather than $3de_g$ electron [9]) and the Jahn-Teller distortions of the local MnO_6 octahedron. This term should also include the breathing model; (v). $H_{hole-hole}$ represents the Coulomb interaction among the $2p$ holes rather than the $3de_g$ electrons.

It is easy to observe that the first three terms in Eq. $(2.1)'$ can cause an indirect exchange interaction between two itinerant $2p$ holes in MnO_2 plane. This indirect interaction is mediated by two nearest neighbour FM or AFM coupling local spins at sites of Mn^{3+} or Mn^{4+} ions (See Fig. 3.2 in Ref. [11].). This indirect interaction is called two local spin-mediated interaction (TLSMI), and can cause Cooper pairing in both macroscopic superconductive state and pseudogap state, in which the systems do not have macroscopic superconductivity in the MnO_2 plane of the high-T_c cuprates [11].

The first three terms of Hamiltonians in Eq. $(2.1)'$ and Eq. (3.5) in Ref. [11] are the same. Using more than fifty pages, Ref. [11] derives the mathematical expression of TLSMI, obtains the solutions of BCS gap equation, gives the numerical program to calculate pseudogap and pairing probability of individual carrier. We can use all the formulas in Ref. [11], and just in the stage of numerical calculations substitute the values of related parameters of manganites, given in section 3. For $S = 2$ Ref. [11] gives

$$TLSMI = -A\frac{272(cos\theta)^2 N'' J J_K^2}{T^2 + B272 \times 64(cos\theta)^2 J J_K^2/\{1 + C20 J_K^2\}}, \quad (2.2)\ (See\ (3.74)\ and\ many\ related\ formulas\ of\ [11])$$

where $A,\ B,\ , C$ are constants, N'' is determined by the size of the cluster with magnetic order, for long-range magnetic order the size of cluster is infinite, N'' has maximum value 2, the minimum value is $N'' = 1$, and θ is the angle between two nearest neighbour Mn ions in FM coupling case (In AFM case $\theta \equiv 0$.) [11].

The pseudogap functions are of $p-$ and d-wave symmetry for FM and AFM, and give in Eqs. (3.67-68) and Eq. (3.66), respectively [11].

Table 1 lists the thirteen similarities as a summary of this section.

3. Values of parameters of manganites

In this section you can see that the values of related parameters for CMR manganites and high-T_c cuprates are nearly equal. We have to use the values of related parameters of CMR manganites for exact comparisons of data with numerical results. All the values of parameters of CMR manganites can be found in the present available references. Eqs. (5.26-5.35) of Ref. [11] show that J_K is a function of $U_d, \Delta_{eff}, V_\circ$. $\Delta_{eff} = 1.8\ eV$ and $U_d = 6.8\ eV$ [13]. The hopping integral t between Mn^{3+} and Mn^{3+} is 0.2 - 1 eV [9]. We take $t_\circ = 0.5$ eV. Of course, if the on-site Coulomb repulsion energy $U_d = 6.8$ eV, then the Coulomb repulsion energy between Mn^{3+} and Cu^{2-}, $V_\circ$, will much less than 6.8 eV. Referring to the CuO_2 plane of high-T_c cuprates, we take $V_\circ = 1.0$ eV [11]. $J = 0.05$ eV [9]. Bandwidth is 1.8 eV [2]. (for reference: the effective mass of itinerant hole is $m_{eff} = 0.3m_e$, m_e is the electron mass, average free path is 1.44 nm, Fermi velocity is 0.38c, $U_d = 7\ eV$ [7]. $m_{eff} = 3.3m_e$, the average free path is 2.5 nm [2].)

4. Numerical results and explanations for experiments

4.1. Pseudogap

(1). Fig. 1 shows the experimental data of the pseudogap versus temperature for $La_{0.625}Ca_{0.375}MnO_3$.

Explanation: Our theoretical cure in Fig. 1 can quantitatively explain the data well.

(2). Fig. 2 shows the experimental data of the pseudogap versus temperature for $La_{2-2x}Sr_{1+2x}Mn_2O_7$ with $x = 0.4$.

Explanation: Our theoretical cure in Fig. 2 can quantitatively explain the data well.

(3). Refs. [16,1] reported that for the sample $La_{2-2x}Sr_{1+2x}Mn_2O_7$ with $x = 0.4$ at $T > 126$ K the pseudogap is observed in the entire Fermi surface, and there is no zero pseudogap anisotropy.

Explanation: The theory in section 2 indicates that in FM state the pseudogap is of p-wave symmetry. Our numerical simulations show that for $La_{2-2x}Sr_{1+2x}Mn_2O_7$ with $x = 0.4$ in FM state the minimum and maximum pseudogap is along the $Mn - O$ bond and 45° away from $Mn - O$ bond directions, respectively. The ratio is $\Delta(Mn - O)/\Delta(45°) = 0.358/0.626 \neq 0$.

(4). Ref. [2] observed that the pseudogap of $La_{2-2x}Sr_{1+2x}Mn_2O_7$ with $x = 0.4$ is of d-wave symmetry at 20 K other than p-wave symmetry.

Explanation: There is phase transition from pure FM to coexistence of FM and AFM at $15 < T < 40$ K in the MnO_2 plane [9]. Our numerical simulations show that in the same values of parameters the d-wave is much easier to occur than the p-wave. This theoretical result can explain the observed d-wave (other than p-wave) pseudogap at $T = 20$ K.

(5). Many different types of magnetic systems can have pseudogap [11,6].

Explanation: Many quite different types of magnetic systems can have, in principle, the same Hamiltonian structure as the first three terms of Eq. $(2.1)'$ [21,1]. So long as a system has the Hamiltonian liking to the first three terms in Eq. (2.1) and there are some appropriate values of parameters, then this system will have the pseudogap certainly.

4.2. CMR

(1). The data on the temperature dependence of CMR for single crystal $La_{1.2}Sr_{1.8}Mn_2O_7$ at different magnetic fields are reported by Refs. [15,16,9,13], which is shown in Fig. 3.

Explanation: According to Refs. [11,20,6], the motion of Cooper pairs in pseudogap states is free but ranom. Similar to the high-Tc cuprates [11,20,6], we refer CMR completely to the formation to Cooper pairs in the pseudogap state as well. In our calculations for the temperature dependence of CMR at 0 and 5 T, we use the expression of resistivity

$$\rho_{ab} = \rho_0 + \rho_1[1 - Q(T)], \tag{4.1}$$

where $Q(T)$ represents the probability of one individual carrier to become one carrier of a Cooper pair, ρ_0 and ρ_1 represent residual resistivity and resistivity without Cooper pairs, respectively. Due to that we study CMR in $La_{1.2}Sr_{1.8}Mn_2O_7$, we neglect the small temperature dependence of rho_1. Refs. [11,6] have given the formula of $Q(T)$ (See Eq. (2.405) in Ref. [11]. According to Eq. (2.2), our numerical calculations need the experimental magnetization curves at H = 0, 5 T, which are given by Refs. [15-17].The better fitting between the data and our numerical result in Fig. 3 indicates that CMR is really completely caused by the formation of Cooper pairs in $La_{1.2}Sr_{1.8}Mn_2O_7$.

(2). The experiments found that the necessary condition occurring CMR is that the CMR manganites are in FM state [8,9].

Explanation: In FM state, the more stronger the applied field is $\Rightarrow$ the more stronger the FM order is $\Rightarrow$ the stronger the magnetization is $\Rightarrow$ the stronger the pairing potential TLSMI in Eq. (2.2) is $\Rightarrow$ the larger the number of Cooper pairs is $\Rightarrow$ the larger the (negative) CMR is.

(3). The magnitude of CMR is a linear function of square of magnetization around Curie temperature, where the magnetization is small [16].

Explanation: Eq. (2.2) indicates that the Cooper pairing potential is a function of square of magnetization, $\propto (cos\theta)^2$. The first order approximation of Taylor expansion in $\propto (cos\theta)^2$ is proportional to $\propto (cos\theta)^2$. The number of Cooper pairs should be dependent on TLSMI (Refer to Eq. (2.405) in Ref. [11].), and, thus, CMR is dependent on $\propto (cos\theta)^2$ linearly.

(4). The data in Fig. 3 show that all the interplane resistivities are equal approximately to the inplane resistivities plus about 39 Ωcm, correspondingly.

Explanation: The Cooper pairs are formed only in the MnO_2 plane. However, the Cooper pairs can tunnel from one MnO_2 plane to another nearest neighbor MnO_2 plane. The tunnel process is of resistance, and does not be sensitive to temperature. Thus, we obtain $\rho_c = \rho_{ab} + 39\ \Omega cm$, where 39 Ωcm is the tunneling resistivity.

(5). The experimental data of resistivity versus temperature at different pressures from 1 atm to 6.0 GPa in sample $La_{0.33}Ca_{0.67}MnO_3$ show that the pressure causes CMR as well as magnetic field [18]. The variations of lattice constants a and b in the MnO_2 plane are: a=5.4610 and 5.4043, b=5.4750 and 5.4324 $\mathring{A}$ for 1 atm and 5.87 GPa, respectively [18].

Explanations: The larger the pressure is $\Rightarrow$ the shorter the lattice constant is $\Rightarrow$ the larger the value of J in Eq. (2.2) is [19] $\Rightarrow$ the larger the value of

TLSMI is $\Rightarrow$ the larger the number of Cooper pairs $\Rightarrow$ the less the resistivity is.

(6). For $La_{0.625}Ca_{0.375}MnO_3$ $\rho(T = T_{M-I} = 120\ K)/\rho(T = 100\ K) = 30$ at a definite band width, and if the band width reduces, then $\rho(T = T_{M-I} = 240\ K)/\rho(T = 100\ K) = 1000$ [3]. Ref. [16] observed the effect of band width on resistivity.

Explanation: Our numerical calculations for $La_{1.2}Sr_{1.8}Mn_2O_7$ are as follows. $\rho(T = 126\ K)/\rho(T = 100\ K) = 18,\ 25,\ 31$ for band width $W = 1.8, 1.5, 1.2$ eV, respectively.

(7). CMR can occur in thallium manganite pyrochlores ($Tl_2^{3+}Mn_2^{4+}O_7$) without double-exchange [13].

Explanation: Our paring potential of Cooper pair TLSMI in Eq. (2.2) is dependent on J, i. e., Heisenberg interaction, and J_K, i. e., Kondo interaction, and is independent of the double-exchange.

(8). Ref. [13] concluded clearly from experimental facts: "Thus, thallium manganite pyrochlores ($Tl_2^{3+}Mn_2^{4+}O_7$) has neither mixed valence for a double exchange-magnetic interaction nor a Jahn-Teller cation such as Mn^{3+}, which both are known to play an essence role in CMR perovskite materials."

Explanation: Although our new Hamiltonian in Eq. (2.2) can contain Jahn-Teller interaction, in all the above numerical calculations, which give the quantitative explanations for both the pseudogap and CMR, we do not consider the Jahn-Teller term. This fact points out that Jahn-Teller effect for the pseudogap and CMR is not important.

(9). The data for epitaxial film and polycrystalline (3, 14, 24 μm average grain size) of $LaCaMnO$ are that the small grain size leads to (i). High resistivity. (ii). Small CMR [13].

Explanation: (i). The conduction occurs in MnO_2 plane. Therefore, the

less the grain's size is, the larger the tunneling resistivity between two grain's MnO_2 planes is. (ii). Eq. (2.2) indicates the Cooper pairing potential TLSMI is proportional to N''. The less the grain's size is $\Rightarrow$ the less the value of N'' is $\Rightarrow$ the less the value of $N'' \Rightarrow$ the less the TLSMI is $\Rightarrow$ the less the number of Cooper pairs $\Rightarrow$ the less the CMR is.

(10). Although the value of the pseudogap in CMR manganites is much larger than that in the high-T_c cuprates, CMR manganites have not macroscopic superconductivity.

Explanation: Ref. [11] proves that the condition of emergence of macroscopic superconductivity is that Josephson coupling energy $E_J(T)$ between Cooper pairs is large enough and [11]

$$E_J(T) \propto \frac{\Delta(T)}{R_n}. \tag{4.2}$$

For manganites, the resistivity without the Cooper pairs, $\rho_{n,manganites}$, is nearly equal to $100 \times \rho_n$, where ρ_n is the resistivity of high-T_c cuprates in normal state. Although the pseudogap $\Delta_{manganites}$ is nearly equal to $10 \times \Delta_{cuprates}$, due to small $E_J(T)$ the maganites never have macroscopic superconductivity. Along this line, it is not impossible that in future one will discovery room temperature macroscopic superconductivity by making a magnetic material with large pseudogap but small resistivity at room temperature .

5. Conclusions

From the thirteen similarities in electronic, lattice, and Hamiltonian structures of CMR manganites with the high-T_c cuprates, we infer that the pseudogaps and CMR of manganites are caused by the formation of Cooper pairs. This inference on Cooper pair's existence in CMR manganites are further verified by the uniform and quantitative explanations for the 15 experimental

facts about the pseudogap and CMR. Therefore, this paper concludes: (1). The observed d- and p-wave symmetry pseudogap in FM and AFM regions, respectively, of CMR manganites come from Cooper pairs; (2). The Cooper pair consists of two oxygen $2p\sigma$ holes, and exists in the MnO_2 plane; (3). The motion of Cooper pairs is random but free; (4). CMR is caused by the free motion of Cooper pairs; (5). The new Hamitonian in Eq. $(2.1)'$ should become a starting point of theoretical study on CMR manganites. One should abandon many Hamiltonians to describe CMR manganites, proposed before this paper, for example in Ref. [9].

6. Six properties of Cooper pairs in CMR manganites

Sections 2, 3, 4, and 5 show that the properties of Cooper pairs in CMR manganites are same as that of the Cooper pairs in the pseudogap state of the high-T_c cuprates at $T_c < T < T^*$.

(i). The free motion has critical velocity

$$v_c = \frac{\Delta}{\hbar k_F}, \tag{6.1}$$

where Δ, $\hbar$, and k_F are pseudogap, Planck constant, and Fermi wavenumber, respectively.

(ii). The motion satisfies Newton equation, if velocity of Cooper pair is less than v_c;

(iii). Do not have Meissner effect, and thus have body current other than surface current;

(iv). Carriers = Cooper pairs + single particles;

(v). The effective resistance does not produce Joule heat;

(vi). For FM, field enhances Cooper pairing potential TLSMI.

7. Applications of CMR manganites

We call any body with pseudogap pseudogapbody. Many applications of the high-T_c cuprates have been given in Refs. [6,11,22,20]. This section gives the application of CMR manganites in energy aspect.

7.1. Applications in energy

7.1.1. Permanent current and permanent strong magnet

A permanent current in a ring made by $La_{0.625}Ca_{0.375}MnO_3$ can be induced by the change of magnetic flux in the ring at room temperature [22,6]. Set the radius of the ring is 0.5 m, and the radius of rings wire is 3 mm. The induction critical current in this ring is $I_c = 2.94 \times 10^8$ A, the inductance is $L = 3.37 \times 10^{-6}$ H, $B_{maximum} = LI_c/(\pi 0.5^2) = 1279$ T in the opening of the ring, the maximum magnetic pressure between the two such rings and at very small distance is $P_{mag-pre} = 6.36 \times 10^{10}$ Pa, and, thus, the maximum magnetic levitation is 5.2×10^9 kg, and so big value of $B_{maximum}$ can storage energy $4.0\times^{11}$ J$/m^3$. If we use the high-T_c cuprates to make the same size ring working at 77 K, then the supercurrent is in the ring's surface with thickness 100 nm due to Meissner effect [23], and, thus $I_c = 1.96 \times 10^3 << 2.94 \times 10^8$ A. If the high-T_c cuprates are hard superconductors, then $I_c = 1.96 \times 10^5$ A. It is important to note that in magnetic field the d-wave superconductivity of the high-T_c cuprates and the p-wave superconductivity of CMR manganites are reduced and increased, respectively.

7.1.2. Power transmission

It is well known that Resistivity of wire made by $La_{0.625}Ca_{0.375}MnO_3$ is [3]

$$\rho(300K) = 1.4 \times 10^{-3}\Omega cm. \tag{7.1}$$

Let us calculate that due to free motion of Cooper pairs, the effective resistivity at 300 K.

(i). $v_c = 2.06 \times 10^6$ cm/second. Thus, critical kinetic energy $E_{critical} = 2.3$ meV.

(ii). We apply voltage on the two ends of a transmission wire $U_{applied} = 2.3$ mV. $U_{applied}$ will accelerate Cooper pairs in the transmission wire. Average velocity of these Cooper pairs $v_{average} = v_c/2$. Thus, average current density $J_{average} = J_c/2$.

At last, we have

$$\rho_{effective}(300K) = \frac{U_{applied}}{J_{average} \times Length)}. \tag{7.2}$$

If $Length = 1\ km = 10^5$ cm, $\rho_{effective}(300K) = 4.6 \times 10^{-17}\Omega$ cm.

Besides little, due to that the applied voltage is used just for acceleration of Cooper pairs, there are no any generation of Joule heat.

There is a sharp question that why all measurements from 1950 to 2014 indicate: manganites are high resistance materials? For example, for $La_{0.625}Ca_{0.375}MnO_3$, $\rho(300K) = 14 \times 10^{-3}\Omega$ cm>> $\rho_{effective}(300K) = 4.6 \times 10^{-17}\Omega$ cm.

Actually, the answer is very simple. Now available four point probes to measure resistivity give following standard data for a wafer of thickness 500 nm, made by $La_{0.625}Ca_{0.375}MnO_3$: At first, the constant current is $I = 4.5$ mA; Then, the voltage is $V = 68$ mV; We obtain $\rho(300K) = 4.53 \times t \times I/V = 14 \times 10^{-3}\Omega$ cm. We know that the critical voltage, i. e., breaking voltage of Cooper pairs, is less than 2.3 mV. Therefore, the Cooper pairs are definitely cannot exist in the wafer, because the Cooper pairs are broken. So, we get high resistivity of manganites. Therefore, we have to abandon the four point probes.

We design the following "small and constant voltage method". Assume

that our sample is made by $La_{0.625}Ca_{0.375}MnO_3$, length=2 cm, thickness t=100 μm, wide=1 cm. At first, we apply constant (!!!) voltage U=2.3 mV, then from Eq. (7.2) $\rho_{effective}(300K) = 2.3 \times 10^{-12}$ Ω cm$<<$ 14×10^{-3} Ω cm.

7.2. Applications in electronic device

7.2.1. Light-emitting devices (generator, mixer, ...)

Principle of light-emission by Josephson tunneling junction: In Fig. 4 the left Cooper electron pair tunnels to the right, obtains energy $2|e|$V due to its free motion. This process is energy-nonconservative. To keep energy conservation this Cooper pair emits one photon with energy $\hbar\nu = 2|e|$V, and returns to the left [11,6].

Therefore, using, for example, $La_{0.625}Ca_{0.375}MnO_3$ to make Manganite-Insulator-Manganite tunneling junction, one can easily obtain photons from very long wavelength to visible light at 300 K by just changing the voltage applied. Actually, many kinds of weak connections have this effect as well[11].

7.2.2. Light-detecting devices

Principle of light-detect by CMR manganites: One Cooper pair absorbs one photon with energy $> 2 \times 250$ meV (for $La_{0.625}Ca_{0.375}MnO_3$), breaks, and becomes two quasiparticles other than just one quasiparticle in semiconductor. Therefore, the sensitivity of light-detector of CMR manganites is higher than that of semiconductors.

7.2.3. Schottky barrier solar cell

Principle of Schottky solar cell: Incident photons produce carriers in semiconductor or CMR manganites, these carriers will move due to Schottky barrier between metal and semiconductor or CMR manganite.

Set $\eta = conversion\ efficiency\ of\ light\ to\ electricity$. For example, band gap of n-Si=1.12 eV. Pseudogap of $La_{0.625}Ca_{0.375}MnO_3$=0.25 eV. There are three reasons that $\eta_{n-Si} << \eta_{LCMO}$.

(i). Semiconductor and $La_{0.625}Ca_{0.375}MnO_3$ absorb one photon produce one and two quasiparticles, respectively. This factor demands $\eta_{n-Si} = 0.5\eta_{LCMO}$;

(ii). Due to the difference of scale of gap, n-Si and $La_{0.625}Ca_{0.375}MnO_3$ absorb ≈3/4 and ≈4/4 of solar spectrum, respectively;

(iii). $\eta \propto Light{-}absorbing\ coefficient\ G \propto (E = E_g)^{1/2}$. For $La_{0.625}Ca_{0.375}MnO_3$ $E_g = 0.5$ eV. For n-Si $E_g = 1.12$ eV. A rough estimation gives:

$$\frac{G_{La_{0.625}Ca_{0.375}MnO_3}}{G_{n-Si}} = \frac{(2-0.5)^{1/2}}{(2-1.12)^{1/2}} = 1.305. \tag{7.3}$$

Now, the best expectation value of η_{n-Si} is 25%. Thus, from (i), (ii), and (iii),

$$\eta_{LCMO} = 25\% \times 2 \times \frac{1.305}{0.75} = 87\%. \tag{7.4}$$

8. Summary on applications of CMR manganites

From the discussions in section 7 we can see the advantages of CMR manganites over semiconductors and superconductors. Tables 2 and 3 give the comparisons.

From Table 2 and 3 we can see that the applications of CMR manganites will bring a new times of material science and material engineering.

New times= =Times of microscopic superconductivity

=Times of Cooper pairs

=Times of pseudogapbody

=Times of CMR manganites

=90% and 80% in applications of superconductors and semiconductors,

will be substituted by CMR manganites, respectively, in future 30 years.

Main reasons for the last equality are: Superconductors need to work, at lest at present, at 77 K, while CMR manganites can work at 300 K; Semiconductor devices produce Joule heat, while CMR manganites do not.

Acknowledgement

The author would like to thank his friend Pai-ying Li for her supports and encouragements in a long time.

References

[1] D. S. Dessau *et al.*, Phys. Rev. Lett. 81 (1998) 192.

[2] N. Mannella *et al.*, Nature, 438 (2005) 474.

[3] U. R. Singh *et al.*, J. Phys.: Condens. Matter, 21 (2009) 355001.

[4] J. Kim *et al.*, Phys. Rev. Lett. 110 (2013) 217203. arxiv.org/pdf/1303.0244.

[5] F. Massee *et al.*, Nature Physics, 7 (2011) 978.

[6] Fu-sui Liu, *Advanced Quantum Mechanics upon Theotems*, (Nova, New Yourk, February 2014).

[7] Y.D. Chuang and D.S. Dessau, in *The Electronic Structure, Fermi Surface, and Pseudogap in Manganites*, Ed, T. Chatterji, (Kluwer academic publishers, Dordrecht, 2004), pp. 93-129.

[8] E. Dagotto, New J. Phys. 7 (2005) 67.

[9] E. Dagotto, *Nanoscale Phase Separation and Colossal MagnetoResistance*, (Springer, Berlin, 2003), p. 118, 81, 15, 16, 122, 86, 27, 335, 46, 47, 315, 84, 74, 21, 17.

[10] D. F. Dionne, *Magnetic Oxides*, (Spronger, Berlin, 2009), p. 98.

[11] Fu-sui Liu, *Genaral Theory of Superconductivity*, (Nova, New York, 2008), p. 95, 111, 163.

[12] Y. -D, Chuang *et al.*, Science, 292 (2001) 1509.

[13] C. N. R. Rao and B. Raveau, *Colossal Magnetoresistance, Charge Ordering and Related Properties of Manganese Oxide*, (World Scientific, Singapore, 1998), p. 281, 340, 207, 194.

[14] C. Sen*et al.*, Phys. Rev. Lett. 105 (2012) 097203.

[15] Y. Moritomo, A. Asamitsu, H. Kuwahara, Y. Tokura, Nature, 380 (1996) 380

[16] Y. Tokura, "Colossal Magnetoresistive Oxides", (Gordon and Breach Publishers, New York, 2000), p. 149, 45, 18, 89.

[17] C. H. Shen and R. S. Liu, Journal of Appl. Phys. 86 (1999) 2178.

[18] Zhiqiang Chen, "Probing spin, chage, and lattice coupling in manganites". PhD thesis, New Jersey Institute of Technology, USA, 2008, 7, 92-95.

[19] Haifen Li, "Synthesis of CMR manganites and ordering phenomena in complex transition metal oxides". PhD thesis, Rheinisch-Westf?lischen Technischen Hochschule Aachen, Germany, 2008, 18.

[20] Fei Tan and Fu-sui Liu, J. Superconductivity and novel magnetism, 25, (2012) 299.

[21] H. Matsukawa and H. Fukuyama, J. Phys. Soc. Jpn. 58 (1989) 2845.

[22] Fu-sui Liu, Journal of Superconductivity and novel magnetism, 25 (2012) 215.

[23] The page 147 in Ref. [6] concluded that the Cooper pairs in the pseudogap state does have Meissner effect. This conclusion is wrong, because one cannot deduce from common velocity that there is common phase of the Cooper pairs in the pseudogap state.

[24] W. Bukel and R. Kleiner, *Superconductivity*, (Wiley-VCH, Tubingen, 2004), p. 12.

[25] P. J. Lee, *Engineering of Superconductivity*, (John Wiley & Sons, New York, 2001).

[26] Zhaoshun Gao, Yanwei Ma et al., Scientific Reports, 2 (2012) 998. DOI: 10.1038/srep00998.

[27] P. Tixador, *Superconducting magnetic energy storage*, in *High Temperarure Superconductors (HTS) for Energy Applications*, Ed. by Ziad Melhem, (Woodhead Publishing, Cambridge, 2012), p. 294.

[28] Xinwei Zhang, et al., *Studies on High Temperature Superconductivity*, (Sichuan Education, Chengdu, 1989), p. 389.

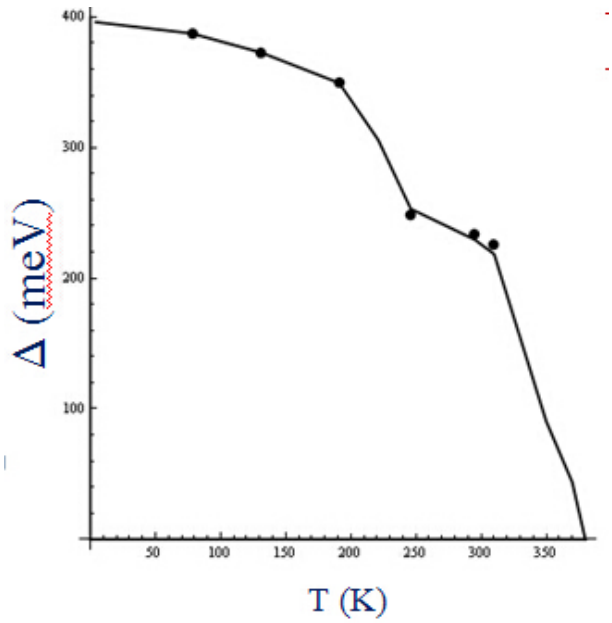

Figure 1: Diagram of pseudogap Δ (meV) versus temperature T (K) for $La_{0.625}Ca_{0.375}MnO_3$. The data come from Ref. [3].

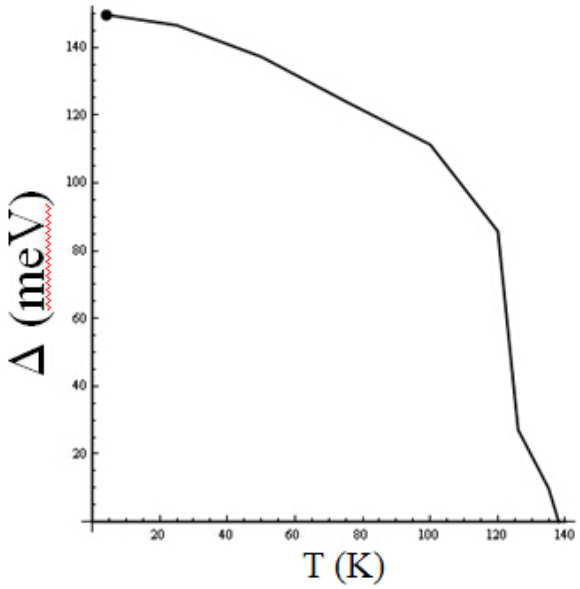

Figure 2: Diagram of pseudogap Δ (meV) versus temperature T (K) for $La_{1.2}Sr_{1.8}Mn_2O_7$. The data come from Ref. [5].

Table 1: The thirteen similarities between CMR manganites and high-T_c cuprates in aspects of lattice, electronic, and Hamiltonian structures

High-T_c cuprates		CMR manganites
Perovskite type-like structure	1	Perovskite type-like structure
CuO_2 plane	2	MnO_2 plane
In CuO_2 plane lattice constant ≈0.39 Å	3	In MnO_2 plane lattice constant ≈0.39 Å
In CuO_2 plane local spin of Cu ions	4	In MnO_2 plane local spin of Mn ions
Carriers are $O_{p\sigma}$ holes	5	Carriers are $O_{p\sigma}$ holes
$O_{p\sigma}$ holes are in CuO_2 plane	6	$O_{p\sigma}$ holes are in MnO_2 plane
Nesting Fermi surface in CuO_2 plane	7	Nesting Fermi surface in MnO_2 plane
High-T_c cuprates		CMR manganites
Strong correlation Hamiltonian in $O_{p\sigma}$ is in Eqs. (2.1) and (2.1)'	8	Strong correlation Hamiltonian in $O_{p\sigma}$ is in Eqs. (2.1) and (2.1)'
Kondo Hamiltonian between hole and local spin$\propto J_K$	9	Kondo Hamiltonian between hole and local spin$\propto J_K$
Heisenberg Hamiltonian between local spins $\propto J$	10	Heisenberg Hamiltonian between local spins $\propto J$
Two local spin-mediated interaction (TLSMI)in Fig. 1.	11	Two local spin-mediated interaction (TLSMI) in Fig. 1.
Formula of TLSMI in Eq. (2.2)	12	Formula of TLSMI in Eq. (2.2)
Pseudogap $T_c < T < T^*$	13	Pseudogap $0 < T < T^*$

Table 2: The contrasts of CMR manganites with semiconductors

Semiconductors		CMR manganites
6 weakness		6 advantages
Produce Joule heat	1	not produce Joule heat
Low number density ($\approx 10^{16}/cm^3$)	2	High number density ($\approx 10^{21}/cm^3$)
Absorb one photon, produce one carrier	3	Absorb one photon, produce two carriers
No Josephson effrect	4	Josephson effect
Not easy to get small band gap	5	Easy to get small band gap
Best transformation time $\tau = 10^{-13}$ S	6	Best transformation time $\tau = 10^{-15}$ S [28]
1 advantage		1 weakness
Can have large band gap, such as $\beta - Ga_2O_3$=4.9 eV	1	Cannot have large band gap, such as the biggest pseudogap¡1 eV

Table 3: The contrasts of CMR manganites with superconductors

Superconductors		CMR manganites
5 weakness		5 advantages
Cannot work at 300 K	1	Can work at 300 K
Surface current	2	Body current
Field reduces current density	3	Field enhances current density
Cannot have large pseudogap at 300 K	4	Can have large pseudogap at 300 K
The smallest transformation time $\tau = 1 \times 10^{-14}$ second	5	The smallest transformation time $\tau = 1 \times 10^{-15}$ second
1 advantage		1 weakness
Josephson effect in magnetic field	1	No Josephson effect in magnetic field

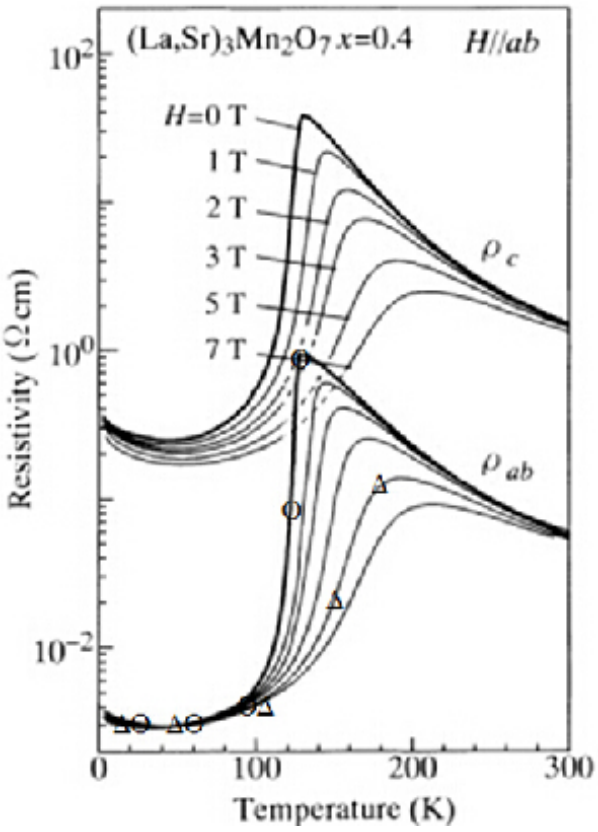

Figure 3: Diagram of data curves [15,16] and theory values for $La_{1.2}Sr_{1.8}Mn_2O_7$. [15,16]. Circles and triangles are numerical results for 0 and 5 T, respectively. Field is parallel to MnO_2 plane. ρ_{ab} and ρ_c are the inplane and interplane resistivity.

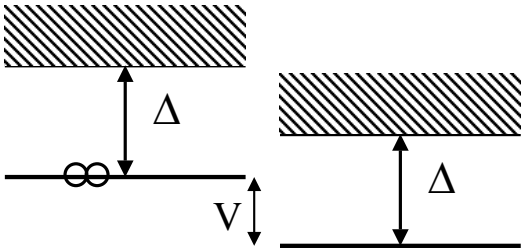

Figure 4: Diagram of energy level of Josephson junction. (The applied Voltage V $\leq$ breakdown voltage $\approx 1 - 2$ eV [11].)